

Magnetic order in thin films of the heavy fermion superconductor UNi_2Al_3

M. Jourdan^{1,a}, A. Zakharov¹, A. Hiess², T. Charlton³, N. Bernhoeft⁴, and D. Mannix⁵

¹ Institut für Physik, Johannes Gutenberg-Universität, Staudingerweg 7, 55128 Mainz, Germany

² Institut Laue Langevin, B.P. 156, 38042 Grenoble Cedex 9, France

³ Rutherford Appelton Laboratory, ISIS facility, Chilton, Didcot, Oxfordshire OX11 0QX, UK

⁴ Dépt. de Recherche Fond. sur la Matière Condensée, CEA-Grenoble, 38054 Grenoble Cedex 9, France

⁵ XMaS UK CRG beamline, ESRF, B.P. 220, 38043 Grenoble Cedex 9, France

Received 19 September 2005

Published online 23 December 2005 – © EDP Sciences, Società Italiana di Fisica, Springer-Verlag 2005

Abstract. Resonant magnetic X-ray scattering was employed to investigate the magnetic state of epitaxial a^* oriented thin films of the heavy fermion superconductor UNi_2Al_3 . The observed incommensurate propagation vector as well as the Néel temperature correspond to those of bulk samples. The 1200 Å film shows magnetic order with a correlation length >800 Å parallel to the growth axis. Out of the three possible magnetic domains the one with the moment direction perpendicular to the film surface is not realized.

PACS. 74.70.Tx Heavy-fermion superconductors – 75.25.+z Spin arrangements in magnetically ordered materials (including neutron and spin-polarized electron studies, synchrotron-source X-ray scattering, etc.) – 74.78.Db Low- T_c films

The heavy fermion superconductors UPd_2Al_3 ($T_{sc} = 2$ K) [1] and UNi_2Al_3 ($T_{sc} = 1$ K) [2] both exhibit the coexistence of superconductivity and magnetic order at low temperatures. However, they display important differences key to the understanding of the interplay between magnetism and superconductivity, an area of active debate in condensed matter physics. Whereas for UPd_2Al_3 there is evidence for a magnetic Cooper-pairing interaction [3–5], the mechanism of superconductivity in UNi_2Al_3 remains open.

Although UNi_2Al_3 is isostructural (hexagonal, $P6mm$) with UPd_2Al_3 , its magnetic and superconducting properties are quite different. In UPd_2Al_3 commensurate magnetic order described with a propagation vector $Q_{\text{UPA}} = (0, 0, 1/2)$ is observed below $T_N = 14$ K. The ordered moments are about $0.85\mu_B$ at low T and lie parallel to a [6]. In UNi_2Al_3 the magnetic ordering temperature is lower, $T_N = 5$ K, the moment smaller, $\mu \simeq 0.2\mu_B$, and the magnetic structure as determined in bulk single crystals has an incommensurate propagation vector $Q_{\text{UNA}} = (\pm 1/2 \pm 0.11, 0, 1/2)$ [7,8]. This magnetization density wave is amplitude modulated with the magnetic moments parallel to a^* [9]. Intriguingly the superconducting properties also appear to be different: in contrast with UPd_2Al_3 there are indications for a superconducting spin triplet state in UNi_2Al_3 [10]. Thus a different unconventional superconducting pairing mechanism may be realized in this compound and the

magnetic properties of these samples are crucial to an understanding of the origin of superconductivity.

Recently we have been able to prepare superconducting epitaxial thin films of UNi_2Al_3 which grow with the a^* -axis perpendicular to the substrate surface and the b - and c -axes within the film plane [11]. For the present experiments we used a film of 1200 Å thickness grown by molecular beam epitaxy. On account of the small sample volume, X-ray resonant magnetic scattering is the experimental method of choice to investigate the temperature dependence of the microscopic magnetic properties. The resonant cross section exploits the sensitivity to the magnetic polarization of the electric dipole excitation of an inner shell electron into magnetically polarized intermediate states [12]. The experiments were performed on the XMaS-CRG beamline (BM28) at the European Synchrotron Radiation Facility (ESRF) with the photon energy tuned to the uranium M_4 absorption edge ($E \simeq 3.73$ keV) in σ - π geometry [13].

At low temperatures magnetic scattering has been observed at $(2, 0.39, 1/2)$ (see inset of Fig. 1) and with reduced intensity at $(1, 1.39, 1/2)$ proving that there is spatial magnetic order in the studied film at least on the resonant probe time scale (10^{-15} – 10^{-14} s). The observed position corresponds to the propagation vector reported of the bulk. On the other hand we did not observe any magnetic scattering peaks at the $(1/2 \pm 0.11, 0, 1/2)$ and $(1.39, 0, 1/2)$ positions. A magnetic peak will be extinct

^a e-mail: jourdan@uni-mainz.de

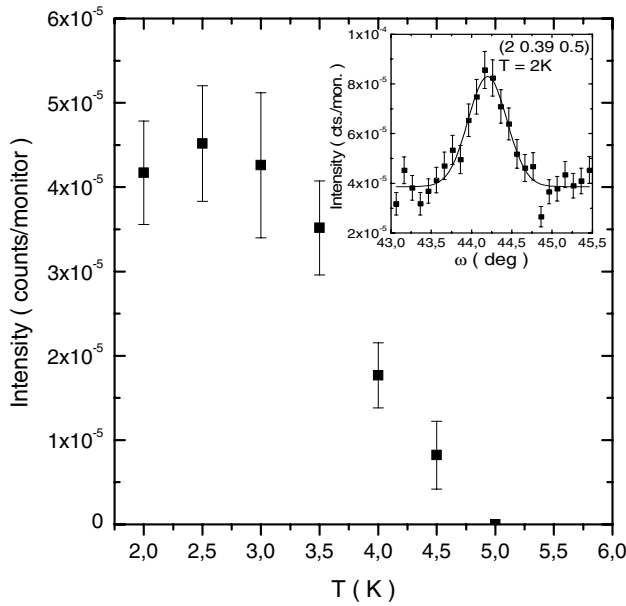


Fig. 1. Temperature dependence of the integrated scattering intensity of ω -scans (see inset) of the magnetic Bragg-peak $Q_m = (2, 0.39, 1/2)$.

when there is no projection of the magnetic moment on the scattered vector at the selected position [13]. However, given the off specular geometry, this condition is not met by all magnetic peaks on the form $(h, 0, 1/2)$ simultaneously. Thus an alternative explanation is proposed: Within the hexagonal plane of UNi_2Al_3 there are three equivalent crystallographic directions resulting in the formation of three magnetic domains. Since each of these domains is associated with a different magnetic ordering wave vector, $(\pm 1/2 \pm 0.11, 0, 1/2)$, $(0, \pm 1/2 \pm 0.11, 1/2)$ and $(\pm 1/2 \pm 0.11, \mp 1/2 \mp 0.11, 1/2)$, at any given magnetic Bragg position scattering arises from only one magnetic domain. Thus the lack of $(h, 0, 1/2)$ intensity can be explained by the absence of magnetic domains with moment direction perpendicular to the film surface. In these experiments we observed magnetic scattering from the second domain only, in which the moment direction is rotated by 60° with respect to the film normal. The third domain was not accessible with our goniometer geometry.

The temperature dependence of the integrated intensity of the magnetic Bragg peak $(2, 0.39, 1/2)$ is shown in Figure 1. The UNi_2Al_3 1200 Å film orders magnetically below $T_N = (4.7 \pm 0.2)$ K, the same temperature where the resistivity curve $R(T)$ shows a kink and increases the magnitude of its slope with decreasing temperature [11].

In general, from the width of Bragg reflections information about the correlation lengths of the sample can be obtained (the longitudinal coherence length of the incident photon is $> 1 \mu\text{m}$). Assuming a constant X-ray intensity in the scattering volume, the scattered amplitude of a finite lattice is proportional to the Fourier transform of a product of three spatial functions given by the lattice periodicity, the atomic group of the unit cell and the exterior shape of the crystal. The exterior shape is described by

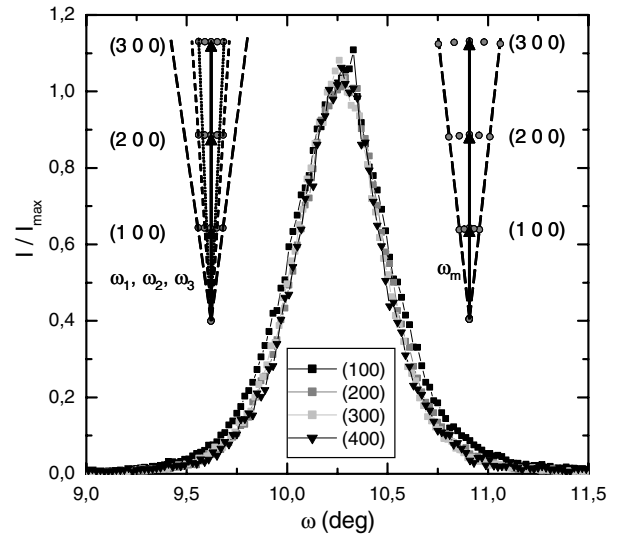


Fig. 2. ω -scans of the specular $(H, 0, 0)$, $H = 1, 2, 3, 4$ peaks of a 1200 Å UNi_2Al_3 thin film. The ω axis of the higher order peaks are shifted to display the scans on top of each other. (measured with a standard 2-circle diffractometer, Cu-anode). Right inset: Schematic representation of the peak broadening due to mosaic spread. Left inset: Schematic representation of the peak broadening due to a finite correlation length within the film plane.

the form function $\sigma(\mathbf{x})$ which is equal to unity inside the sample volume and zero outside with the Fourier transform $\Sigma(\mathbf{s})$. The corresponding reciprocal space is given by the set of functions $\Sigma(\mathbf{s})$ repeated around each node of the reciprocal lattice extending to infinity [14]. Thus the broadening of the reciprocal lattice points Δq_i due to correlation length ℓ_i or finite size effects in a given direction can be estimated by $\Delta q_i \simeq 2\pi/\ell_i$. However, the basic assumption that the X-ray intensity is constant within the sample volume is inconsistent with the resonant nature of the scattering process which results in an intensity fall off within the thin film [15]. This reduces the effective scattering volume and alters the relevance of $\Delta q_i \simeq 2\pi/\ell_i$ to a lower bound of the correlation length.

A sometimes dominant contribution to the peak width is obtained from crystal mosaic spread. In epitaxial thin films with island growth mode mosaic spread arising from a distribution of tilting angles ω_m of the crystallite axes perpendicular to the substrate is a common feature. This generates spherical-shell segments in reciprocal space centered at the origin of the specular reciprocal lattice vector with dimensions depending on the scattering order (see right inset of Fig. 2).

On the other hand correlation length effects due to atomic disorder or finite size effects generate a broadening which is the same for all points in reciprocal space (see left inset of Fig. 2). Thus rocking curves (ω -scans) of specular Bragg reflections of increasing order have the same ω -width if the broadening is dominated by the mosaic spread and a decreasing width if the broadening is due to correlation length effects. In Figure 2 rocking curves

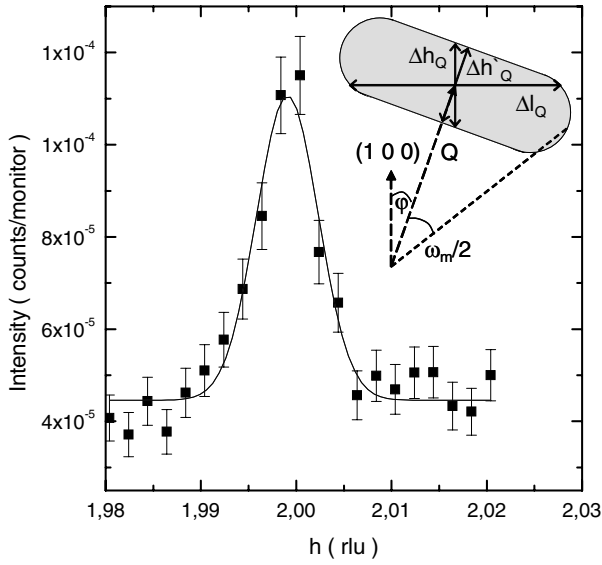


Fig. 3. Scan parallel to the a^* -axis around the magnetic Bragg position $Q_m = (2, 0.39, 1/2)$ of UNi₂Al₃ ($T = 2$ K). Inset: Schematic representation of the influence of mosaicity and finite correlation length on the peak broadening in reciprocal space (see text).

of the $(H, 0, 0)$ peaks ($H = 1, 2, 3, 4$) are shown. For $H > 2$ no dependence of the curve width on H is observable, the $(1, 0, 0)$ curve is only slightly broader than the other curves. Thus the broadening of the structural reciprocal space points is dominantly due to the crystal mosaicity with the angular full width at half height of $\omega_m \simeq 0.42^\circ$.

Once the effects of the crystal mosaic structure have been taken into account, the width of the magnetic reflections can be discussed in the framework of the magnetic correlation length. The magnetic scattering vectors of the UNi₂Al₃ thin films are off-specular with an angle φ between the film normal $(1, 0, 0)$ and the scattering vector Q . For the magnetic peak $Q_m = (2, 0.39, 0.5)$ we obtain $\phi = 16.6^\circ$. Thus for an h -scan of Q_m the measured h -width Δh_{Q_m} is similar to the pure correlation length broadening (rlu: reciprocal lattice units): $\Delta h'_{Q_m} = \Delta h_{Q_m} \cdot \cos \phi = (0.0062 \pm 0.0005)\text{rlu} \cdot 0.96 = (0.0059 \pm 0.0005)\text{rlu}$ (see Fig. 3).

From this a magnetic correlation length of $\ell_{m,h} = (|a| \cos 30^\circ) / \Delta h'_{Q_m} > (760 \pm 60)\text{\AA}$ is calculated. Thus the UNi₂Al₃ thin films show magnetic order in the a^* -direction (the direction of the surface normal) with a correlation length which exceeds the lower limit (400\AA , [7]) estimated for bulk single crystals. At the same wavelength the structural peak $Q_s = (2, 0, 1)$ has a similar correlation length $\ell_{s,h} > (800 \pm 15)\text{\AA}$.

Given the film thickness of $d = (1200 \pm 50)\text{\AA}$ as determined from rate monitors during the growth process these lower bounds suggest a magnetic and structural correlation which extends over the complete film thickness.

For the determination of the magnetic in plane correlation lengths of the epitaxial thin film scans of Q_s and

Q_m along the c axis (l -scan) and a axis were performed. However, the peaks are strongly broadened in these directions due to the mosaic spread (broadening for the l -scan: Δl_Q , see inset of Fig. 3). The measured widths are consistent with this mosaicity and no additional broadening is necessary to describe the data within the error of our experiment. Only a lower bound for the magnetic correlation length, independent of the direction in the film plane, of $\ell_{m,in-plane} > 500\text{\AA}$ can be given.

Concluding, epitaxial thin films of UNi₂Al₃ exhibit the same type of incommensurate antiferromagnetic order as bulk samples. The magnetic correlation length $\ell > 800\text{\AA}$ estimated from resonant magnetic X-ray scattering exceeds the lower boundary obtained from neutron scattering experiments on bulk samples. The formation of a magnetic domain with a moment direction perpendicular to the film surface seems to be energetically unfavorable, possibly since it would imply an uncompensated magnetic moment.

XMaS is an EPSRC-funded project. Financial support by the German Research Foundation (DFG) is acknowledged.

References

1. C. Geibel, C. Schank, S. Thies, H. Kitazawa, C.D. Bredel, A. Böhm, M. Rau, A. Grauel, R. Caspary, R. Helfrich U. Ahlheim, G. Weber, F. Steglich, Z. Phys. B **84**, 1 (1991)
2. C. Geibel, S. Thies, D. Kaczorowski, A. Mehner, A. Graul, B. Seidel, U. Ahlheim, R. Helfrich, K. Petersen, C.D. Bredel, F. Steglich, Z. Phys. B **83**, 305 (1991)
3. N. Bernhoeft, N. Sato, B. Roessli, N. Aso, A. Hiess, G.H. Lander, Y. Endoh, T. Komatsubara, Phys. Rev. Lett. **81**, 4244 (1998)
4. M. Jourdan, M., Huth, H. Adrian, Nature **398**, 47 (1999)
5. N.K. Sato, N. Aso, K. Miyake, S. Shiina, P. Thalmeier, G. Vareloggiannis, C. Geibel, F. Steglich, P. Fulde, T. Komatsubara, Nature **410**, 340 (2001)
6. L. Paolasini, J.A. Paixao, G.H. Lander, P. Burlet, N. Sato, T. Komatsubara, Phys. Rev. B **49**, R7072 (1994)
7. A. Schröder, J.G. Lussier, B.D. Gaulin, J.D. Garrett, W.J.L. Buyers, L. Rebersky, S.M. Shapiro, Phys. Rev. Lett. **72**, 136 (1994)
8. N. Aso, B. Roessli, N. Bernhoeft, R. Calemczuk, N.K. Sato, Y. Endoh, T. Komatsubara, A. Hiess, G.H. Lander, H. Kadowaki, Phys. Rev. B **61**, R11 867 (2000)
9. A. Hiess, P.J. Brown, E. Lelievre-Berna, B. Roessli, N. Bernhoeft, G.H. Lander, N. Aso, N.K. Sato, Phys. Rev. B **64**, 134413 (2001)
10. K. Ishida, D. Ozaki, T. Kamatsuka, H. Tou, M. Kyogaku, Y. Kitaoka, N. Tateiwa, N.K. Sato, N. Aso, C. Geibel, F. Steglich, Phys. Rev. Lett. **89**, 037002 (2002)
11. M. Jourdan, A. Zakharov, M. Foerster, H. Adrian, Phys. Rev. Lett. **93**, 097001 (2004)
12. J.P. Hannon, G.T. Trammell, M. Blume, D. Gibbs, Phys. Rev. Lett. **61**, 1245 (1988)
13. J.H. Hill, D.F. McMorrow, Acta Cryst. **A52**, 236 (1996)
14. e.g.A. Guinier, *X-Ray Diffraction In Crystals, Imperfect Crystals and Amorphous Bodies* (Dover Publications, New York 1994), p. 90
15. N. Bernhoeft, Acta Cryst. A **55**, 274 (1999)